

Safe Sequential Path Planning of Multi-Vehicle Systems Under Presence of Disturbances and Imperfect Information

Somil Bansal*, Mo Chen*, Jaime F. Fisac, and Claire J. Tomlin

Abstract—Recently, there has been an immense surge of interest in using unmanned aerial vehicles (UAVs) for civil purposes. Multi-UAV systems are safety-critical, and safety guarantees must be made to ensure no undesirable configurations such as collisions occur. Hamilton-Jacobi (HJ) reachability is ideal for analyzing such safety-critical systems because it provides safety guarantees and is flexible in terms of system dynamics; however, its direct application is limited to small-scale systems of no more than two vehicles because of the exponential-scaling computation complexity. By assigning vehicle priorities, the sequential path planning (SPP) method allows multi-vehicle path planning to be done with a computation complexity that scales linearly with the number of vehicles. Previously the SPP method assumed no disturbances in the vehicle dynamics, and that every vehicle has perfect knowledge of the position of higher-priority vehicles. In this paper, we make SPP more practical by providing three different methods for accounting for disturbances in dynamics and imperfect knowledge of higher-priority vehicles. Each method has advantages and disadvantages with different assumptions about information sharing. We demonstrate our proposed methods in simulations.

I. INTRODUCTION

Recently, there has been an immense surge of interest in using unmanned aerial vehicles (UAVs) for civil purposes. The applications of UAVs extend well beyond package delivery, and include aerial surveillance, disaster response, and other important tasks [1], [2], [3], [4], [5]. Many of these applications will involve UAVs flying in an urban environment, potentially in close proximity of humans. As a result, government agencies such as the Federal Aviation Administration (FAA) and National Aeronautics and Space Administration (NASA) of the United States are urgently trying to develop new scalable ways to organize an air space in which potentially thousands of UAVs can fly [6], [7].

One essential problem that needs to be addressed is how a group of vehicles in the same vicinity can reach their destinations while avoiding collision with each other. Several previous studies have attempted to address this problem. In some of these studies, specific control strategies for the vehicles or moving entities are assumed, and approaches such as induced velocity obstacles have been used [8], [9], [10]. Other researchers have used ideas involving virtual potential

fields to maintain collision avoidance while maintaining a specific formation [11], [12]. Although interesting results emerge from these previous studies, simultaneous trajectory planning and collision avoidance are not considered.

In the past, trajectory planning and collision avoidance problems in safety-critical systems have been studied using reachability analysis, which provides guarantees on the success and safety of optimal system trajectories [13], [14], [15], [16], [17]. In reachability analysis, one computes the reachable set, defined as the set of states from which the system can be driven to a target set. Reachability analysis has been successfully used in applications involving systems with no more than two vehicles, such as pairwise collision avoidance [14], automated in-flight refueling [18], two-player reach-avoid games [19], and many others [20].

Despite the advantages of reachability analysis, it cannot be directly applied to scenarios involving complex high dimensional systems such as multi-vehicle systems. The computation of reachable sets involves solving a Hamilton-Jacobi (HJ) partial differential equation (PDE) on a grid representing a discretization of the state space, causing an exponential scaling of computation complexity with respect to the dimension of the system, or roughly speaking, with the number of vehicles present.

In this paper, we build on the work in [21], and assume a reasonable structure in the multi-vehicle path planning problem. In the sequential path planning (SPP) scheme, vehicles are assigned some priority. Higher-priority vehicles may ignore the lower-priority vehicles, who must take into account the presence of higher-priority vehicles by treating them as induced time-varying obstacles. Unlike the work in [21], we incorporate disturbances for all vehicles and consider three different assumptions on the information each of the vehicles may have access to, making the sequential path planning substantially more practical. For each of the assumed information patterns, we propose a reachability-based method to compute the induced obstacles that would guarantee collision avoidance as well as successful transit to the destination. We demonstrate and compare our proposed methods through numerical simulations.

II. PROBLEM FORMULATION

Consider N vehicles whose joint dynamics described by the time-varying ordinary differential equation (ODE)

$$\begin{aligned} \dot{x}_i &= f_i(t, x_i, u_i, d_i), \quad t \in [t_i^{\text{EDT}}, t_i^{\text{STA}}] \\ u_i &\in \mathcal{U}_i, d_i \in \mathcal{D}_i \\ i &= 1, \dots, N \end{aligned} \quad (1)$$

This work has been supported in part by NSF under CPS:ActionWebs (CNS-931843), by ONR under the HUNT (N0014-08-0696) and SMARTS (N00014-09-1-1051) MURIs and by grant N00014-12-1-0609, by AFOSR under the CHASE MURI (FA9550-10-1-0567). The research of M. Chen and J. F. Fisac have received funding from the “NSERC” program and “la Caixa” Foundation, respectively.

* Both authors contributed equally to this work. All authors are with the Department of Electrical Engineering and Computer Sciences, University of California, Berkeley. {somil, mochen72, jfisac, tomlin}@eecs.berkeley.edu

where $x_i \in \mathbb{R}^{n_i}$ is the state of the i th vehicle, u_i is the control of the i th vehicle, and d_i is the disturbance experienced by the i th vehicle. In general, the physical meaning of x_i and the dynamics f_i depend on the specific dynamic model of vehicle i , and need not be the same across the different vehicles.

We assume that the control functions $u_i(\cdot)$, $d_i(\cdot)$ are drawn from the set of measurable functions¹, and $f_i(t, x_i, u_i, d_i)$ is bounded, Lipschitz continuous in x_i for any fixed t, u_i, d_i , and measurable in t, u_i, d_i for each x_i . Given any initial state x_i^0 and any control function $u_i(\cdot)$, there exists a unique continuous trajectory $x_i(\cdot)$ solving (1) [22].

Let t_i^{EDT} and t_i^{STA} denote the earliest departure time and scheduled time of arrival, respectively, of vehicle i . Let $p_i \in \mathbb{R}^p$ denote the position of vehicle i ; note that p_i in most practical cases would be a subset of the state x_i . Denote the rest of the states h_i , so that $x_i = (p_i, h_i)$.

Under the worst case disturbance, each vehicle aims to get to some set of target states, denoted $\mathcal{T}_i \subset \mathbb{R}^{n_i}$, at some scheduled time of arrival t_i^{STA} . On its way to \mathcal{T}_i , each vehicle must avoid the danger zones $\mathcal{A}_{ij}(t)$ of all other vehicles $j \neq i$ for all time. In general, the danger zone can be defined to capture any undesirable configuration between vehicle i and vehicle j . In this paper, we define $\mathcal{A}_{ij}(t)$ as

$$\mathcal{A}_{ij}(t) = \{x_i \in \mathbb{R}^{n_i} : \|p_i - p_j(t)\|_2 \leq R_c\}, \quad (2)$$

the interpretation of which is that a vehicle is another vehicle's danger zone if the two vehicles are within a Euclidean distance of R_c apart. The joint path planning problem is depicted in Fig. 1.

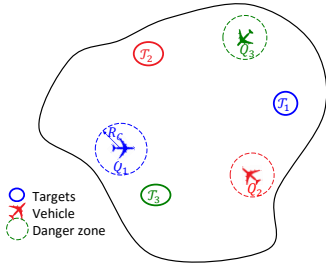


Fig. 1: Problem setup.

The problem of driving each of the vehicles in (1) into their respective target sets \mathcal{T}_i would be in general a differential game of dimension $\sum_i n_i$. Due to the exponential scaling of the complexity with the problem dimension, an optimal solution is computationally intractable even for $N > 2$.

In this paper, we assume assigned priorities of the vehicles as in the SPP method [21]. While traveling to its target set, a vehicle may ignore the presence of lower priority vehicles, but must take full responsibility for avoiding higher priority vehicles. Since the analysis in [21] did not take into account the presence of disturbances d_i and limited

information available to each vehicle, we extend the work in [21] to consider these practically important aspects of the problem. In particular, we answer the following inter-dependent questions that were not previously addressed:

- 1) How can each vehicle guarantee that it will reach its target set without getting into any danger zones, despite the disturbances it experiences?
- 2) How can each vehicle take into account the disturbances that other vehicles experience?
- 3) How should each vehicle robustly handle situations with limited information about the state and intention of other vehicles?

III. SOLUTION VIA DOUBLE-OBSTACLE HJ VI AND SPP

A. Double-Obstacle Hamilton-Jacobi Variational Inequality

Our solution method takes advantage of the double-obstacle HJ variational inequality (VI) [17], in which one computes the backwards reachable set (BRS) $\mathcal{V}(t)$ in the presence of a time-varying target set $\mathcal{T}(t)$ and time-varying obstacle $\mathcal{G}(t)$. Mathematically, we are given a system with state z evolving according to

$$\begin{aligned} \dot{z} &= f(t, z, u, d), \quad t \in [0, T] \\ z(0) &= z_0, \quad u \in \mathcal{U}, d \in \mathcal{D} \end{aligned} \quad (3)$$

After defining some target set $\mathcal{T}(t)$, we compute $\mathcal{V}(t)$, defined by

$$\begin{aligned} \mathcal{V}(t) &= \{z : \exists u \in \mathbb{U}, \forall \gamma[u] \in \Gamma, (3) \\ &\Rightarrow \exists s \in [t, T], z(s) \in \mathcal{T}(s) \wedge z(\tau) \notin \mathcal{G}(\tau) \forall \tau \in [t, s]\} \end{aligned} \quad (4)$$

where \mathbb{U} is the set of measurable functions satisfying control constraints at every t , and Γ is the set of non-anticipative strategies [14] defined as follows:

$$\begin{aligned} \gamma \in \Gamma &:= \{\mathcal{N} : \mathbb{U}_1 \rightarrow \mathbb{U}_2 \mid u_1(r) = \hat{u}_1(r) \text{ a. e. } r \in [t, s] \\ &\Rightarrow \mathcal{N}[u_1](r) = \mathcal{N}[\hat{u}_1](r) \text{ a. e. } r \in [t, s]\} \end{aligned} \quad (5)$$

Informally, the BRS is the set of states from which there exists a control such that for all non-anticipative disturbances, the system is driven into the target set $\mathcal{T}(t)$ in the time horizon $[t, T]$ without first entering the obstacle set $\mathcal{G}(t)$.

Given the target set $\mathcal{T}(t)$ specified as an implicit surface function such that $\mathcal{T}(t) = \{z : l(t, z) \leq 0\}$, the BRS can be obtained as the implicit surface function $V(t, z)$ such that $\mathcal{V}(t) = \{z : V(t, z) \leq 0\}$, where $V(t, z)$ is the viscosity solution [23] to the following HJ VI:

$$\begin{aligned} \max \Big\{ \min \Big\{ D_t V(t, z) + H(t, z, D_z V), l(t, z) - V(t, z) \Big\} \\ - g(t, z) - V(t, z) \Big\} &= 0, \quad t \in [0, T] \\ V(T, x) &= \max \{l(T, x), -g(T, x)\} \\ H(t, z, p) &= \min_{u \in \mathcal{U}} \max_{d \in \mathcal{D}} p \cdot f(t, z, u, d) \end{aligned} \quad (6)$$

where $g(t, x)$ is the implicit surface function representing $\mathcal{G}(t)$: $\mathcal{G}(t) = \{z : g(t, x) \leq 0\}$. After the BRS is computed,

¹ A function $f : X \rightarrow Y$ between two measurable spaces (X, Σ_X) and (Y, Σ_Y) is said to be measurable if the preimage of a measurable set in Y is a measurable set in X , that is: $\forall V \in \Sigma_Y, f^{-1}(V) \in \Sigma_X$, with Σ_X, Σ_Y σ -algebras on X, Y .

the optimal control can be obtained as follows:

$$u^*(t, z) = \arg \min_{u \in \mathcal{U}} \max_{d \in \mathcal{D}} H(t, z, D_z V) \quad (7)$$

In theory, one could define the state to be the joint states of all vehicles, $z = (x_1, x_2, \dots, x_N)$, define the dynamics (3) to follow (1), the target set \mathcal{T} to correspond to the situation in which all vehicles have arrived at their targets $\mathcal{T}_i, i = 1, \dots, N$, and the obstacle set \mathcal{G} to correspond to the combination of all the danger zones \mathcal{A}_{ij} . Then, (6) could be solved to obtain $\mathcal{V}(t)$, and then the joint optimal control would be given by (7).

However, practically, the dimensionality of the joint state z would be extremely high. In fact, for even the simplest vehicle models, solving (6) would be intractable for more than two vehicles. Therefore, we propose the sequential path planning method, which allows (6) to be solved in the state space of each vehicle, making the computation complexity scale linearly, as opposed to exponentially, with the number of vehicles.

B. Sequential Path Planning

In order to make the N -vehicle path planning problem safe and tractable, we impose a reasonable structure to the problem: each vehicle is assigned a strict priority ordering. When planning its trajectory to its target, a higher-priority vehicle can disregard the presence of a lower priority vehicle. In contrast, a lower priority vehicle must take into account the presence of all higher priority vehicles, and plan its trajectory in a way that avoids the higher priority vehicles' danger zones. For convenience and without loss of generality, let vehicle i have the i th highest priority and denote it as Q_i .

Optimal path planning in this setting is enabled by a HJ VI which computes the BRS $\mathcal{V}_i(t)$ from a target set \mathcal{T}_i in the presence of time-varying obstacles $\mathcal{G}_i(t)$. In the sequential path planning application, the time-varying obstacles represent regions of the state space of Q_i that must be avoided in order to ensure that Q_i does not enter any danger zones of higher priority vehicles. We present three different ways to compute \mathcal{G}_i , obstacles induced by higher priority vehicles in Section IV. For now, we proceed assuming \mathcal{G}_i is given.

To obtain the optimal control for reaching the target we adapt (6) to Q_i and solve the following HJ VI:

$$\begin{aligned} \max \left\{ \min \left\{ D_t V_i(t, x_i) + H_i(t, x_i, D_{x_i} V), \right. \right. \\ \left. \left. l_i(t, x_i) - V_i(t, x_i) \right\}, -g_i(t, x_i) - V_i(t, x_i) \right\} = 0, \\ t \in [t^{\text{EDT}}, t^{\text{STA}}] \\ V_i(t^{\text{STA}}, x_i) = \max \{ l_i(x_i), -g_i(t^{\text{STA}}, x_i) \} \\ H_i(t, x_i, p) = \min_{u_i \in \mathcal{U}_i} \max_{d_i \in \mathcal{D}_i} p \cdot f(t, x_i, u_i, d_i) \end{aligned} \quad (8)$$

Here, the target set \mathcal{T}_i , obstacle set $\mathcal{G}_i(t)$, and BRS $\mathcal{V}_i(t)$ are related to $l_i(x_i), g_i(t, x_i), V_i(t, x_i)$ as follows:

$$\begin{aligned} \mathcal{T}_i &= \{x_i : l_i(x_i) \leq 0\} \\ \mathcal{G}_i(t) &= \{x_i : g_i(t, x_i) \leq 0\} \\ \mathcal{V}_i(t) &= \{x_i : V_i(t, x_i) \leq 0\} \end{aligned} \quad (9)$$

From the BRS, the optimal control for vehicle Q_i is then given as

$$u_i^*(t, x_i) = \arg \min_{u_i \in \mathcal{U}_i} H_i(t, x_i, D_{x_i} V_i) \quad (10)$$

If Q_i uses the optimal control given by (10), then Q_i can be guaranteed to reach the target \mathcal{T}_i as long as Q_i departs by the latest departure time t_i^{LDT} , defined as $\inf_t V_i(t, x_i) \leq 0$.

IV. OBSTACLE GENERATION

Obstacles can be generated in many different ways depending on the assumptions made about the information the vehicles have about each other. In each of the three obstacle generation methods that we present, the goal is to compute, for each lower priority vehicle Q_i , the time-varying obstacle induced by each higher priority vehicle $Q_j, j < i$, denoted by $\mathcal{O}_i^j(t)$. Once $\mathcal{O}_i^j(t)$ is computed, we can then solve (8) with the union of all obstacles induced by higher priority vehicles as the total obstacle set $\mathcal{G}_i(t)$:

$$\mathcal{G}_i(t) = \bigcup_{j=1}^{i-1} \mathcal{O}_i^j(t) \quad (11)$$

In general, the different methods of obstacle generation can be used in a single path planning problem, since different control strategies can be assumed for each vehicle independently. This means that $\mathcal{O}_i^j(t)$ can be computed using a different method for each j . For example, a more predictable vehicle may induce obstacles under the stronger assumptions in Section IV-A, while a vehicle that requires more control freedom may induce obstacles under the weaker assumptions in Section IV-B.

A. Method 1: Centralized Controller

In this obstacle generation method, the induced obstacle for a vehicle Q_j is computed assuming that Q_j is applying the optimal control $u_j^*(t, x_j)$ given by (10), which takes Q_j to the target in the optimal way according to the value function $V_j(t, x_j)$. If there is a centralized controller directly controlling each of the N vehicles, then the control law of each vehicle can be enforced. In this case, lower priority vehicles can safely assume that higher priority vehicles are applying the enforced control law.

From the perspective of a lower priority vehicle Q_i , a higher priority vehicle $Q_j, j < i$ induces an time-varying obstacle that represents the positions that could possibly be within the capture radius R_c of Q_j given that Q_j is executing the feedback controller $u_j^*(t, x_j)$. Determining this obstacle involves first solving a forward reachability problem. The solution gives us the forward reachable set (FRS) of Q_j starting from its initial state $x_j(t^{\text{EDT}})$ at initial time t^{EDT} , denoted $\mathcal{W}_j(t)$ and defined as follows:

$$\begin{aligned} \mathcal{W}_j(t) &= \{y \in \mathbb{R}^{n_j} : \dot{x}_j = f_j(x_j, u_j^*(t, x), d_j) \\ &\Rightarrow \forall d_j \in \mathcal{D}_j, x_j(t) = y\} \end{aligned} \quad (12)$$

Conveniently, FRSs can be computed using a modified version of (8), defined in (13):

$$\begin{aligned}
D_t V_j(t, x_j) + H_j(t, x_j, D_{x_j} V) &= 0, t \in [t_j^{\text{EDT}}, t_j^{\text{STA}}] \\
V_j(t_j^{\text{STA}}, x_j) &= l_j(x_j) \\
H_j(t, x_j, p) &= \min_{u_j \in \mathcal{U}_j} \min_{d_j \in \mathcal{D}_j} p \cdot f(t, x_j, u_j, d_j)
\end{aligned} \tag{13}$$

where l is chosen to be such that $\mathcal{T} = \{x_j(t_0)\}$. In practice, when there is uncertainty in the initial state of Q_j , we set \mathcal{T}_j to be a small region around $x_j(t_0)$. To impose that the optimal control is used, we substitute $u_j = u_j^*(t, x_j)$ into (13) instead of minimizing over u_j .

The FRS $\mathcal{W}_j(t)$ represents the set of possible states at time t of a higher-priority vehicle Q_j given the worst case disturbance $d_j(\cdot)$ and given that Q_j uses the feedback controller $u_j^*(t, x)$. In order for a lower-priority vehicle Q_i to guarantee that it does not go within a distance of R_c to Q_j , Q_i must stay a distance of at least R_c away from the set $\mathcal{W}_j(t)$ for all possible values of the non-position states h_j . This gives the obstacle induced by a higher priority vehicle Q_j for a lower priority vehicle Q_i as follows:

$$\mathcal{O}_i^j(t) = \{x_i : \text{dist}(p_i, \mathcal{P}_j(t)) \leq R_c\} \tag{14}$$

where the $\text{dist}(\cdot, \cdot)$ function represents the minimum distance from a point to a set, and the set $\mathcal{P}_j(t)$ is the set of states in the FRS $\mathcal{W}_j(t)$ projected onto the states representing position p_j , and disregarding the non-position dimensions h_j :

$$\mathcal{P}_j(t) = \{p : \exists h_j, (p, h_j) \in \mathcal{W}_j(t)\}. \tag{15}$$

B. Method 2: Least Restrictive Control

If there is no centralized controller to enforce the control policy for higher priority vehicles, weaker assumptions must be made by the lower priority vehicles to ensure collision avoidance. One reasonable assumption that a lower priority vehicle can make is that all higher priority vehicles follow the least restrictive control that would take them to their targets. This control would be given by

$$u_j \in \begin{cases} \{u_j^*(t, x_j) \text{ given by (10)}\} & \text{if } u \in \partial \mathcal{V}_i(t), \\ \mathcal{U}_i & \text{otherwise} \end{cases} \tag{16}$$

Such a controller allows each higher priority vehicle to use any controller it desires, except when it is on the boundary of the BRS, $\partial \mathcal{V}_i$, in which case the optimal control $u_j^*(x_j)$ given by (10) must be used to get to the target on time. This assumption is the weakest assumption that could be made by lower priority vehicles given that the higher priority vehicles will get to their targets on time.

Suppose a lower priority vehicle Q_i assumes that higher priority vehicles $Q_j, j < i$ use the least restrictive control strategy (16). From the perspective of the lower priority vehicle Q_i , a higher priority vehicle Q_j could be in any state that is reachable from Q_j 's initial state $x_j(t^{\text{EDT}})$ and from which the target \mathcal{T}_j can be reached. Mathematically, this is defined by Q_j is the intersection of the FRS from the initial state $x_j(t^{\text{EDT}})$ and the BRS defined in (4) from the target

set \mathcal{T}_j , $\mathcal{V}_j(t) \cap \mathcal{W}_j(t)$. In this situation, since Q_j cannot be assumed to be using any particular feedback control, $\mathcal{W}_j(t)$ is defined in (17) and can also be computed by solving (13).

$$\begin{aligned}
\mathcal{W}_j(t) &= \{y \in \mathbb{R}^{n_j} : \exists u \in \mathcal{U}, \exists d \in \mathcal{D}, \\
&\quad \dot{x}_j = f_j(x_j, u_j, d_j) \Rightarrow x_j(t) = y\}
\end{aligned} \tag{17}$$

In turn, the obstacle induced by a higher priority Q_j for a lower priority vehicle Q_i is as follows:

$$\mathcal{O}_i^j(t) = \{x_i : \text{dist}(p_i, \mathcal{P}_j(t)) \leq R_c\} \tag{18}$$

where $\mathcal{P}_j(t)$ is given by

$$\mathcal{P}_j(t) = \{p : \exists h_j, (p, h_j) \in \mathcal{V}_j(t) \cup \mathcal{W}_j(t)\} \tag{19}$$

C. Method 3: Robust Tracking of Nominal Trajectories

A third way of computing induced obstacles is to have vehicles commit to approximately tracking a robustly feasible nominal trajectory obtained in the path-planning phase. If a vehicle can be guaranteed to track a trajectory with a bounded error at all times, then this bound can be used to determine the induced obstacle. The planning phase does not make full use of the vehicle's control authority, as some margin is needed to reject unexpected disturbances. Therefore, with this method, planning is done for a reduced control set $\mathcal{U}^p \subset \mathcal{U}$ according to Section III.

In this context, robust nonlinear control techniques such as Lyapunov-based methods [24] can be used to compute robust "funnels" around a concrete nominal trajectory. In this paper, we use reachability to determine the tracking error bound so that the tracking error bound can be determined independently of the nominal trajectory.

Here, we wish to find a robust controlled-invariant set in the joint state space of the vehicle and a tracking reference that may "maneuver" arbitrarily over time, and in the presence of an unknown bounded disturbance. Taking a worst-case approach, the tracking reference can be viewed as a virtual evader vehicle that is optimally avoiding the actual vehicle to enlarge the tracking error. We therefore can model trajectory tracking as a pursuit-evasion game in which the actual vehicle is playing against the coordinated worst-case action of the virtual vehicle and the disturbance. In general, this game will be governed by dynamics of the form:

$$\begin{aligned}
\dot{x} &= f(t, x, u, d), \\
\dot{x}_r &= f(t, x_r, u_r, 0), \\
u &\in \mathcal{U}, u_r \in \mathcal{U}^p, d \in \mathcal{D}, \\
t &\in [0, T].
\end{aligned} \tag{20}$$

Given an error bound $\mathcal{E}(x_{r,i})$ on the tracking error $e = x - x_r$, we define the target set \mathcal{T} for this reachability problem to be the set of joint configurations where this bound is violated: $\mathcal{T} = \{(x, x_{r,i}) : x \notin \mathcal{E}(x_{r,i})\}$. In this case, the BRS $\mathcal{V}(t)$ represents the set of states from which the vehicle may be driven to violate the tracking error bounds, outside of $\mathcal{E}(x_{r,i})$.

With analogous definitions as those in Section III, $\mathcal{V}(t)$ can be characterized as the negative region of the solution V to a simpler case of (6):

$$\begin{aligned} \min \{ & D_t V(t, z) + H(t, z, D_z V), l(t, z) - V(t, z) \} = 0, \\ & t \in [0, T], \\ & V(T, z) = l(T, z), \\ & H(t, z, p) = \max_{u \in \mathcal{U}} \min_{u_r \in \mathcal{U}^p} \min_{d \in \mathcal{D}} p \cdot f_z(t, z, u, u_r, d), \end{aligned} \quad (21)$$

where for compactness of notation we denote $z = (x, x_r)$ and $f_z(t, z, u, u_r, d) = [f(t, x, u, d), f(t, x_r, u_r, 0)]$. The complement of $\mathcal{V}(0)$ is the maximal robust controlled-invariant set in \mathcal{T}^c . Letting $T \rightarrow \infty$ we obtain the infinite controlled-invariant set, which we denote by Ω . If this set is nonempty, then the tracking error e at flight time is guaranteed to remain within \mathcal{E} provided that the vehicle starts inside Ω and subsequently applies the feedback control law implicitly defined in (21):

$$\kappa(x, x_r) \in \arg \max_{u \in \mathcal{U}} \min_{u_r \in \mathcal{U}^p, d \in \mathcal{D}} D_z V(0) \cdot f_z(t, z, u, u_r, d). \quad (22)$$

In cases where the error dynamics are independent of the absolute state as in (23), Ω can be computed in the state space of the tracking error e to produce a feedback control law that also only depends on e , which significantly reduces the problem dimensionality.

$$\begin{aligned} \dot{e} &= f_e(t, e, u, u_r, d), \\ u &\in \mathcal{U}, u_r \in \mathcal{U}^p, d \in \mathcal{D}, \\ t &\in [0, T], \end{aligned} \quad (23)$$

Given \mathcal{E} , we can guarantee that Q_i will reach its target \mathcal{T}_i if $\mathcal{E} \subset \mathcal{T}_i$; thus, in the path planning phase, we modify \mathcal{T}_i to be $\{x : \mathcal{E}(x) \subseteq \mathcal{T}_i\}$.

Finally, since each vehicle Q_i can only be guaranteed to stay within $\mathcal{E}(x_{r,i})$, we must make sure at any given time, the error bounds of Q_i and Q_j , $\mathcal{E}(x_{r,i})$ and $\mathcal{E}(x_{r,j})$, do not intersect. This can be done by choosing the induced obstacle to be the Minkowski sum of the error bounds:

$$\mathcal{O}_i^j(t) = \mathcal{E}(0) + \mathcal{E}(x_{r,j}(t)) \quad (24)$$

where the 0 denotes the origin.

V. NUMERICAL SIMULATIONS

We demonstrate our proposed methods using a four-vehicle example. Each vehicle has the following simple kinematics model:

$$\begin{aligned} \dot{p}_{x,i} &= v_i \cos \theta_i + d_{x,i} \\ \dot{p}_{y,i} &= v_i \sin \theta_i + d_{y,i} \\ \dot{\theta}_i &= \omega_i + d_{\theta,i}, \\ \underline{v} \leq v_i \leq \bar{v}, |\omega_i| &\leq \bar{\omega}, \\ \|(d_{x,i}, d_{y,i})\|_2 \leq d_r, |d_{\theta,i}| &\leq \bar{d}_\theta \end{aligned} \quad (25)$$

where $p_i = (p_{x,i}, p_{y,i})$ represent vehicle Q_i 's position, θ_i represents Q_i 's heading, and $d = (d_{x,i}, d_{y,i}, d_{\theta,i})$ represent

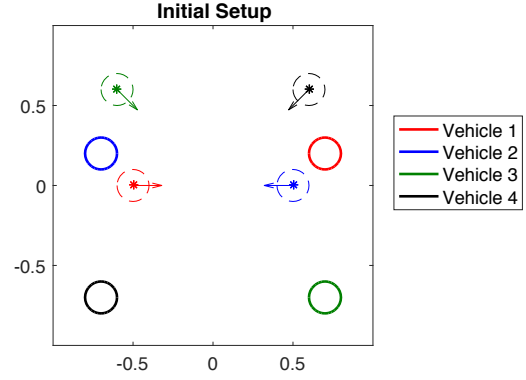


Fig. 2: Initial configuration of the four-vehicle example.

the disturbances in the three states. The disturbance bounds are chosen as $d_r = 0.1$ and $\bar{d}_\theta = 0.2$. The control of Q_i is $u_i = (v_i, \omega_i)$, where v_i is the speed of Q_i and ω_i is the turn rate; both controls have a lower and upper bound. For illustration purposes, we chose $\underline{v} = 0.5, \bar{v} = 1, \bar{\omega} = 1$; however, our method can easily handle the case in which these inputs differ across vehicles and cases in which each vehicle has different dynamic models.

The initial states of the vehicles are given as follows:

$$\begin{aligned} x_1^0 &= (-0.5, 0, 0), \\ x_2^0 &= (0.5, 0, \pi), \\ x_3^0 &= (-0.6, 0.6, 7\pi/4), \\ x_4^0 &= (0.6, 0.6, 5\pi/4). \end{aligned} \quad (26)$$

Each of the vehicles have a target set \mathcal{T}_i that is circular in their position p_i centered at $c_i = (c_{x,i}, c_{y,i})$ with radius r :

$$\mathcal{T}_i = \{x_i \in \mathbb{R}^3 : \|p_i - c_i\| \leq r\} \quad (27)$$

For the example shown, we chose $c_1 = (0.7, 0.2), c_2 = (-0.7, 0.2), c_3 = (0.7, -0.7), c_4 = (-0.7, -0.7)$ and $r = 0.1$. The setup of the example is shown in Fig. 2.

Since the joint state space of this system is intractable for a direct application of HJ reachability theory, we repeatedly solve (6) to compute BRSs from the targets $\mathcal{T}_i, i = 1, 2, 3, 4$, in that order, with moving obstacles induced by vehicles $j = 1, \dots, i-1$. We also obtain $t_i^{\text{LDT}}, i = 1, 2, 3, 4$ assuming $t_i^{\text{STA}} = 0$ without loss of generality. Note that even though t_i^{STA} is assumed to be same for all vehicles in this example for simplicity, our method can easily handle the case in which t_i^{STA} are different for each vehicle.

For each proposed method of computing induced obstacles, we show the vehicles' entire trajectories (colored dotted lines), and overlay their positions (colored asterisks) and headings (arrows) at a point in time in which they are in relatively dense configuration. In all cases, the vehicles are able to avoid each other's danger zones (colored dashed circles) while getting to their target sets in minimum time. In addition, we show the evolution of the BRS over time for Q_3 (green boundaries) as well as the induced obstacles of higher-priority vehicles (black boundaries).

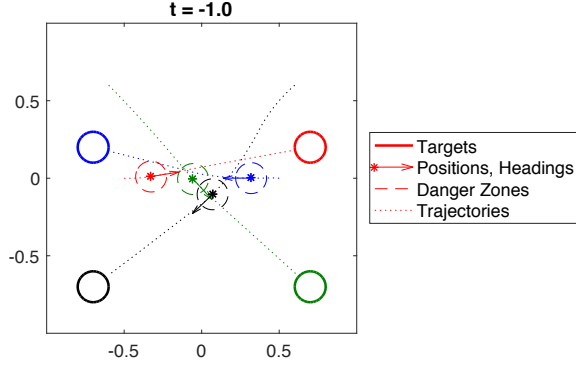


Fig. 3: Simulated trajectories in the centralized controller method. Since the higher priority vehicles induce relatively smaller obstacles in this case, vehicles do not deviate much from a straight line trajectory towards their respective targets.

A. Centralized Controller

Fig. 3 shows the simulated trajectories in the situation where a centralized controller enforces each vehicle to use the optimal controller $u_i^*(t, x_i)$ according to (10), as described in Section IV-A.

In this case, no vehicle appears to deviate slightly from a straight line trajectory towards, just enough to avoid higher priority vehicles. The deviation is small since the centralized controller is quite restrictive, making the possible positions of higher priority vehicles cover a small area. In the dense configuration at $t = -1.0$, the vehicles are close to each other but still outside each other's danger zones.

Fig. 4 shows the evolution of the BRS for Q_3 (green boundary), as well as the obstacles (black boundary) induced by the higher priority vehicles Q_1 (blue) and Q_2 (red). The locations of the induced obstacles at different time points include the actual positions of Q_1 and Q_2 at those times, and the size of the obstacles remains relatively small. t_i^{LDT} numbers for the four vehicles (in order) in this case are $-1.35, -1.37, -1.96$ and -2.04 , respectively. Numbers are relatively close for vehicles Q_1, Q_2 and Q_3, Q_4 , because the obstacles generated by higher priority vehicle are small and hence does not affect t^{LDT} of the lower priority vehicles significantly.

B. Least Restrictive Control

Fig. 5 shows the simulated trajectories in the situation where each vehicle assumes that higher priority vehicles use the least restrictive control to reach their targets, as described in IV-B. Fig. 6 shows the BRS and induced obstacles for Q_3 .

Q_1 (red) takes a relatively straight path to reach its target. From the perspective of all other vehicles, large obstacles are induced by Q_1 , since lower priority vehicles make the weak assumption that higher priority vehicles are using the least restrictive control. Because the obstacles induced by higher priority vehicles are so large, it is faster for lower priority vehicles to wait until higher priority vehicles pass by than to move around the higher priority vehicles. As a result, the

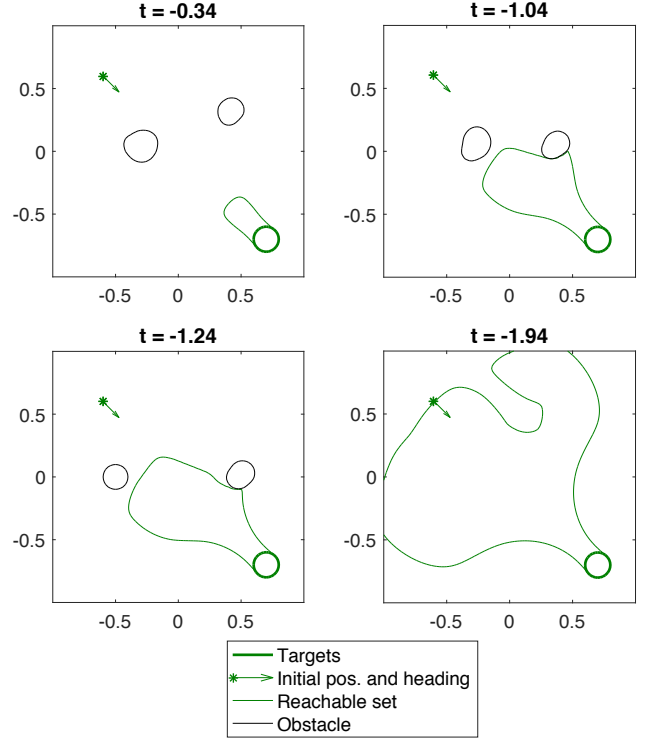


Fig. 4: Evolution of the BRS and the obstacles induced by Q_1 and Q_2 for Q_3 in the centralized controller method. Since every vehicle is applying the optimal control at all times, the obstacle sizes are relatively small.

vehicles never form a dense configuration, and their trajectories are all relatively straight, indicating that they end up taking a short path to the target after higher priority vehicles pass by. This is also indicated by low t_i^{LDT} numbers for the four vehicles, which are $-1.35, -1.97, -2.68$ and -3.39 , respectively. Note that, compared to the centralized controller method, t_i^{LDT} s decrease significantly for all vehicles, except Q_1 for which the number does not change as it is the highest priority vehicle, and hence need not account for any moving obstacles.

From Q_3 's (green) perspective, the large obstacles induced by Q_1 and Q_2 are shown in Fig. 6 as the black boundary. As the BRS (green boundary) evolves over time, its growth gets inhibited by the large obstacle for a long time, from $t = -0.89$ to $t = -1.39$. Eventually, the boundary of the BRS reaches the initial state of the green vehicle at $t = t_i^{\text{LDT}} = -2.66$.

C. Robust Trajectory Tracking

Fig. 7 shows the vehicle trajectories in the situation where each vehicle tracks a pre-specified trajectory and is guaranteed to stay inside a "bubble" around the trajectory. Fig. 8 shows the evolution of BRS and induced obstacles for vehicle Q_3 . The obstacles induced by other vehicles inhibit the evolution of the BRS, carving out thin channels, which can be seen at $t = -2.63$, that separate the BRS into different

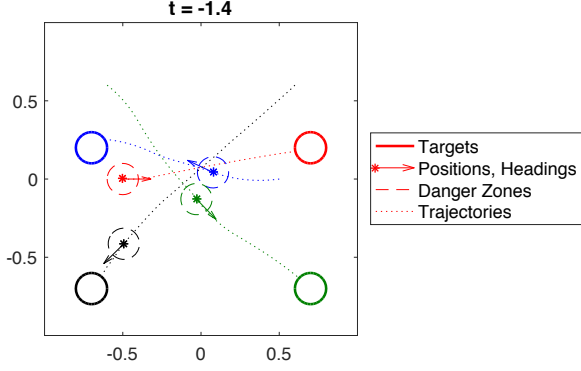


Fig. 5: Simulated trajectories in the least restrictive control method. All vehicles start moving before Q_1 starts, because the large obstacles make it optimal to wait until higher priority vehicles pass by, leading to a smaller t_i^{LDT} .

islands. One can see how these channels and islands form by examining the time evolution of the BRS set.

t_i^{LDT} numbers for the four vehicles in this case are $-1.63, -3.16, -3.63$ and -2.49 respectively. In this method, vehicles use reduced control authority for path planning towards a reduced-size effective target set. As a result, higher-priority vehicles tend to have higher t_i^{LDT} compared with the other two methods, as seen by t_1^{LDT} . Because of the sacrifice in higher-priority vehicles' path planning process, in some cases the t_i^{LDT} of lower priority vehicles may increase, as evident from t_4^{LDT} . Overall, it is unclear whether t_i^{LDT} for a particular vehicle would increase or decrease compared to the other methods, as t_i^{LDT} is increased by conservative path planning by higher-priority vehicles, and decreased by conservative path planning of Q_i .

VI. COMPARISON OF PROPOSED METHODS

This section briefly discusses the relative advantages and limitations of the proposed obstacle generation methods. Each method makes a trade-off between optimality (in terms of t_i^{LDT}) and flexibility in control and disturbance rejection.

A. Centralized Controller

Given an order of priority, the vehicles will have the relatively high t_i^{LDT} in this method since a higher-priority vehicle maximizes its t_i^{LDT} as much as possible, while at the same time inducing a relatively small obstacle as to minimize its impedance towards the lower-priority vehicles. A limitation of this method is that a centralized controller is likely required to ensure that the optimal control is being applied by the vehicles at all times, and hence safety.

B. Least Restrictive Control

This method gives more control flexibility to the higher priority vehicles, as long as the control does not push the vehicle out of its BRS. This flexibility, however, comes at the price of having larger induced obstacle, lowering t_i^{LDT} for the lower-priority vehicles.

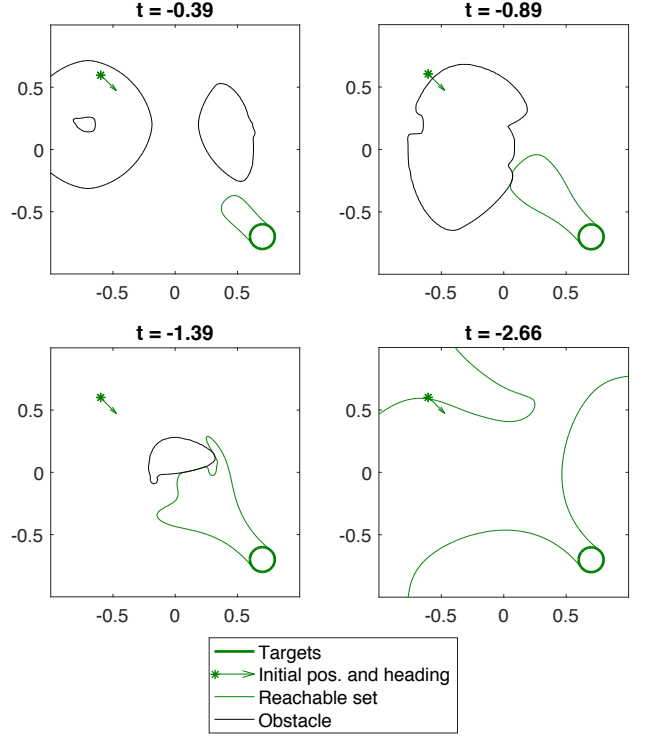


Fig. 6: Evolution of the BRS for Q_3 in the least restrictive control method. t_3^{LDT} is significantly lower than that in the centralized controller method (-1.96 vs. -2.68), reflecting the impact of bigger induced obstacles.

C. Robust Trajectory Tracking

Since the obstacle size is constant over time, this method is easier to implement from a practical standpoint. This method also aims at striking a balance between t_i^{LDT} across vehicles. In particular, the t_i^{LDT} of a higher priority vehicle can be lower compared to the centralized controller method for example, so that a lower priority vehicle can achieve a higher t_i^{LDT} , making this method particularly suitable for the scenarios where there is no strong sense of priority among vehicles. This method, however, is computationally tractable when the tracking error dynamics are independent of the absolute states, as it otherwise requires doing computation in the joint state space of system dynamics and virtual vehicle dynamics as defined in (20).

VII. CONCLUSIONS AND FUTURE WORK

We have proposed three different methods of generating induced obstacles in the sequential path planning method; these three methods can be used independently across the different vehicles in the path planning problem. In each method, different assumptions about the control strategy of higher-priority are made. In all of the methods, all vehicles are guaranteed to successfully arrive and their respective destinations without entering each other's danger zones despite the worst-case disturbance the vehicles could experience. Compared to the work in [21], our proposed methods result in lower

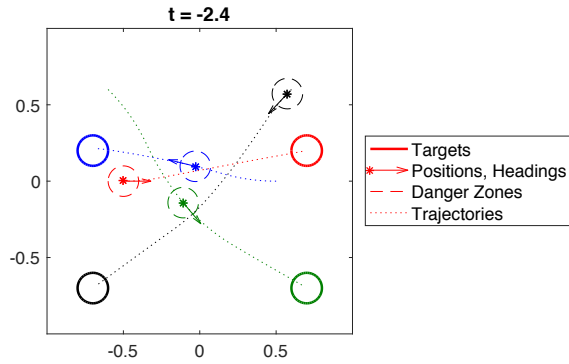


Fig. 7: Simulated trajectories for the robust trajectory tracking method.

vehicle densities so that the vehicles have enough leeway to guarantee safety in the presence of disturbances and limited information. Future work includes exploring methods for fast re-planning, and making the multi-vehicle system robust to unforeseen circumstances such as the presence of intruders.

REFERENCES

- [1] B. P. Tice, "Unmanned aerial vehicles – the force multiplier of the 1990s," *Airpower Journal*, 1991.
- [2] W. M. Debusk, "Unmanned aerial vehicle systems for disaster relief: Tornado alley," in *Infotech@Aerospace Conferences*, 2010.
- [3] Amazon.com, Inc. (2016) Amazon prime air. [Online]. Available: <http://www.amazon.com/b?node=8037720011>
- [4] AUVSI News. (2016) Uas aid in south carolina tornado investigation. [Online]. Available: <http://www.auvsi.org/blogs/auvsi-news/2016/01/29/tornado>
- [5] BBC Technology. (2016) Google plans drone delivery service for 2017. [Online]. Available: <http://www.bbc.com/news/technology-34704868>
- [6] Jointed Planning and Development Office (JPDO), "Unmanned aircraft systems (UAS) comprehensive plan – a report on the nation's UAS path forward," Federal Aviation Administration, Tech. Rep., 2013.
- [7] National Aeronautics and Space Administration. (2016) Challenge is on to design sky for all. [Online]. Available: <http://www.nasa.gov/feature/challenge-is-on-to-design-sky-for-all>
- [8] P. Fiorini and Z. Shiller, "Motion planning in dynamic environments using velocity obstacles," *International Journal of Robotics Research*, vol. 17, pp. 760–772, 1998.
- [9] G. C. Chasparis and J. S. Shamma, "Linear-programming-based multi-vehicle path planning with adversaries," in *Proceedings of American Control Conference*, June 2005.
- [10] J. van den Berg, M. C. Lin, and D. Manocha, "Reciprocal velocity obstacles for real-time multi-agent navigation," in *IEEE International Conference on Robotics and Automation*, May 2008, pp. 1928–1935.
- [11] R. Olfati-Saber and R. M. Murray, "Distributed cooperative control of multiple vehicle formations using structural potential functions," in *IFAC World Congress*, 2002.
- [12] Y.-L. Chuang, Y. Huang, M. R. D'Orsogna, and A. L. Bertozzi, "Multi-vehicle flocking: Scalability of cooperative control algorithms using pairwise potentials," in *IEEE International Conference on Robotics and Automation*, April 2007, pp. 2292–2299.
- [13] E. N. Barron, "Differential Games with Maximum Cost," *Nonlinear analysis: Theory, methods & applications*, pp. 971–989, 1990.
- [14] I. Mitchell, A. Bayen, and C. Tomlin, "A time-dependent Hamilton-Jacobi formulation of reachable sets for continuous dynamic games," *IEEE Transactions on Automatic Control*, vol. 50, no. 7, pp. 947–957, July 2005.
- [15] O. Bokanowski, N. Forcadel, and H. Zidani, "Reachability and minimal times for state constrained nonlinear problems without any controllability assumption," *SIAM Journal on Control and Optimization*, pp. 1–24, 2010.

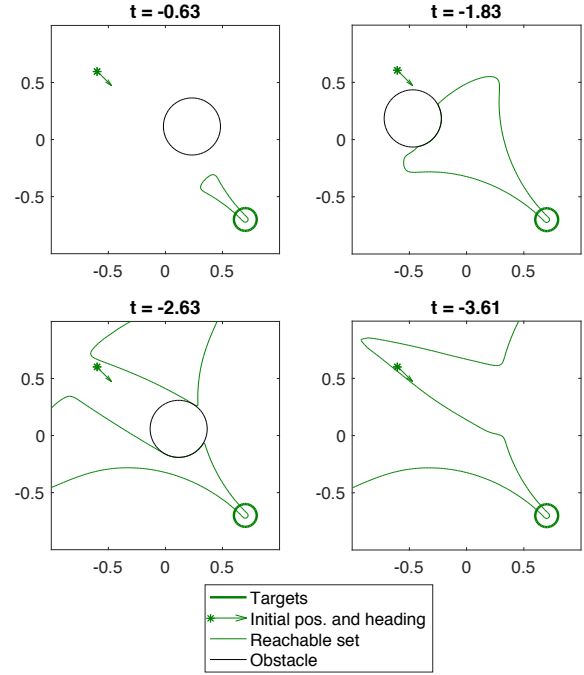


Fig. 8: Evolution of the BRS for Q_3 in the robust trajectory tracking method. As the BRS grows in time, the induced obstacles carve out a channel. The obstacle at $t = -0.63$ and $t = -1.83$ are induced by Q_1 and the obstacle at $t = -2.63$ is induced by Q_2 . Note that a smaller target set is used to compute the BRS to ensure that the vehicle reaches the target set by $t = 0$ for any allowed tracking error.

- [16] K. Margellos and J. Lygeros, "Hamilton-Jacobi Formulation for Reach-Avoid Differential Games," *IEEE Transactions on Automatic Control*, vol. 56, no. 8, Aug 2011.
- [17] J. F. Fisac, M. Chen, C. J. Tomlin, and S. S. Shankar, "Reach-avoid problems with time-varying dynamics, targets and constraints," in *18th International Conference on Hybrid Systems: Computation and Controls*, 2015.
- [18] J. Ding, J. Sprinkle, S. S. Sastry, and C. J. Tomlin, "Reachability calculations for automated aerial refueling," in *IEEE Conference on Decision and Control*, Cancun, Mexico, 2008.
- [19] H. Huang, J. Ding, W. Zhang, and C. Tomlin, "A differential game approach to planning in adversarial scenarios: A case study on capture-the-flag," in *Robotics and Automation (ICRA), 2011 IEEE International Conference on*, 2011, pp. 1451–1456.
- [20] A. M. Bayen, I. M. Mitchell, M. Oishi, and C. J. Tomlin, "Aircraft autoland safety analysis through optimal control-based reach set computation," *Journal of Guidance, Control, and Dynamics*, vol. 30, no. 1, 2007.
- [21] M. Chen, J. Fisac, C. J. Tomlin, and S. Sastry, "Safe sequential path planning of multi-vehicle systems via double-obstacle hamilton-jacobi-isaacs variational inequality," in *European Control Conference*, 2015.
- [22] E. A. Coddington and N. Levinson, *Theory of ordinary differential equations*. Tata McGraw-Hill Education, 1955.
- [23] M. G. Crandall and P.-L. Lions, "Viscosity solutions of Hamilton-Jacobi equations," *Transactions of the American Mathematical Society*, vol. 277, no. 1, pp. 1–42, 1983.
- [24] A. Majumdar and R. Tedrake, *Algorithmic Foundations of Robotics X: Proceedings of the Tenth Workshop on the Algorithmic Foundations of Robotics*. Springer Berlin Heidelberg, 2013, ch. Robust Online Motion Planning with Regions of Finite Time Invariance, pp. 543–558.